PHYSICAL REVIEW B **79**, 113104 (2009)

Density-functional study of the electronic and optical properties of the spinel compound $CuIr_2S_4$

Soumyajit Sarkar, Molly De Raychaudhury, and T. Saha-Dasgupta
S.N. Bose National Centre for Basic Sciences, Kolkata 700098, India

(Received 6 November 2008; revised manuscript received 15 January 2009; published 20 March 2009)

Using first-principles density-functional calculations we have computed the electronic and optical properties of spinel compound $CuIr_2S_4$, which undergoes a structural phase transition, accompanied by a metal-insulator transition at a temperature of about 230 K. The nature of this transition has been discussed in the literature in terms of both the correlated singlet formation picture as well as the orbitally driven Peierls transition picture. Our first-principles calculations find little role of correlation. Our calculated reflectivity and conductivity data for both the high-temperature and low-temperature phases are found to be in good agreement with measured data by Wang *et al.* [Phys. Rev. B **69**, 153104 (2004)].

DOI: 10.1103/PhysRevB.79.113104 PACS number(s): 71.20.Be, 78.20.−e, 71.15.Mb

The metal-insulator transition (MIT) in condensed matter physics has drawn the attention of researchers for decades due to its vast application possibilities following the discovery of high-T_c cuprates[1] and manganites.[2] While the MIT is a commonly occurring phenomenon among transition-metal oxides and sulphides, its origin seems to be varied. The classic example of MIT in the case of V_2O_3 turned out to be caused by correlation induced enhancement of crystal field splitting.[3] The MIT in the case of magnetic Fe_3O_4 (Ref. 4), on the other hand, is believed to be caused by correlation assisted charge-ordering transition between Fe^{+2} and Fe^{+3}.

The spinel compounds with their geometrically frustrated configuration in this context have been discussed in great detail in terms of occurrence of complicated ordering at low temperature with associated MIT from a high-temperature (HT) metallic phase. $CuIr_2S_4$ forms such a compound which has been reported to undergo a first-order MIT near 230 K simultaneous to structural phase transition.[5,6] While the HT phase has a cubic spinel structure with $Fd\text{-}3m$ symmetry, the low-temperature (LT) structure shows a reduction in symmetry. The low-temperature structure was initially characterized to be tetragonal space group[5] $I4_1/amd$, but the study also reported observation of additional Bragg peaks which were unindexed. The refined measurements by Radalli *et al.*[7] using neutrons revealed a fascinating octamer ordering in LT $CuIr_2S_4$ with a triclinic space group. The octamer ordering consists of tetramerization of Ir-Ir bonds with short, long, and intermediate bond lengths giving rise to octamer clusters, one of which exhibits alternation of Ir-Ir bond lengths.[7] The formation of such superstructures has been explained by Croft *et al.*[8] in terms of formation of correlated spin singlet dimers, similar to the case of VO_2.[9] Assuming the divalent state of S ions and monovalent state of Cu which is supported by NMR experiment,[10] the Ir ions occupying octahedral site are nominally in the 3.5+ state, which is a mixed valent state. At low temperature, Ir ions are therefore expected to charge disproportionately into Ir^{3+} ions with completely filled t_{2g} states and Ir^{4+} ions with two full and one 1/2-filled t_{2g} states. It was then interpreted by Croft *et al.* that Ir^{4+} ions with their $S=1/2$ configuration form correlation assisted spin singlets which lead to alternation of Ir^{4+}-Ir^{4+} bond lengths, while Ir^{3+}-Ir^{3+} bond lengths remain uniform. While correlation assisted spin singlet formation is probably valid in the case of 3*d* transition metal based oxide systems such as VO_2 or Ti_4O_7, [11] $CuIr_2S_4$ with Ir being in the 5*d* state and S being in the 3*p* state with more extended wave functions compared to O 2*p* state is expected to give rise to wide bands with much weaker correlation effect. An alternative scenario has been proposed by Khomskii and Mizokawa,[12] in terms of the *orbitally driven Peierls state*. According to this idea, though the spinel structure is a three-dimensional structure, the Ir only sublattice consists of one-dimensional (1D) crisscross chains (see Fig. 3 in Ref. 8). Significant overlap of Ir *d* orbitals aligned along a given chain direction and negligible in other chain directions leads to formation of essentially one-dimensional bands and with proper filling lead to a Peierls-type effect. The measurement of optical spectrum on single crystals[13] conducted on both HT and LT structures conjectured that the changes observed in the optical conductivity and reflectivity spectra between the high-temperature and low-temperature data are essentially caused by the reconstruction of band structure following the structural changes from high temperature to low temperature.

In this Brief Report we study the exact nature of such changes in optical properties in terms of electronic structure calculations, using density-functional theory (DFT) calculations, which to best of our knowledge has not been carried out so far. The calculations have been carried out with no shape approximation to the potential and charge density. The basis has been chosen to be linear augmented plane wave (LAPW) as implemented in WIEN2K code.[14] For the number of plane waves, the criterion used was muffin-tin radius multiplied by $k_{\max}$ (for the plane wave) yielding a value of 7. The number of *k* points used in the irreducible part of the Brillouin zone was 104 for the self-consistent calculation and 256 for the optical calculation.

Figure 1 shows the density of states (DOS) as obtained in generalized gradient approximation (GGA) of the exchange-correlation functional. Focusing on the DOS at the high temperature, we find significant hybridization between delocalized Ir-5*d* and S-3*p* giving rise to wide *d*-*p* hybridized bands spanning the energy range of about 12 eV, from 8 eV below the Fermi energy (E_f) to 4 eV above the Fermi energy. The Cu-*d* derived states localized at an energy of about 2.5 eV below E_f remain completely full in agreement with earlier band-structure calculation[15] and NMR studies.[10] The Ir-*d* projected DOS shows formation of distinct 1D-like features (see inset) at energies close to the Fermi energy (E_f) which

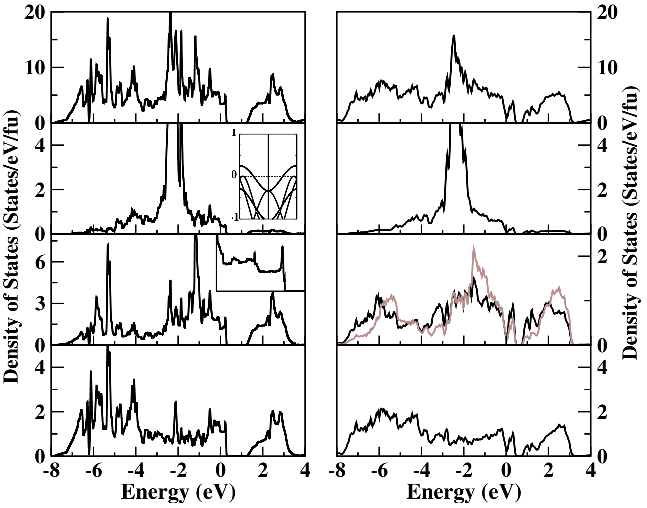

FIG. 1. (Color online) The total and orbital projected density of states of $CuIr_2S_4$ for the high temperature (left panels) and low temperature (right panels), respectively. The panels from top to bottom represent the total DOS, DOS projected on to Cu-*d*, Ir-*d* and S-*p*. The insets in the high-temperature DOS show the band structure and DOS close to E_f exhibiting predominant 1D-like features. The bands have been plotted along the high symmetry directions (011)-(000)-(110). The black and the gray lines in panel corresponding to Ir-*d* projected DOS for the low temperature represent the DOS corresponding the dimerized and undimerized Ir atoms, respectively.

gets merged to a broad filled manifold of Ir t_{2g} states on moving to energies further away from E_f. This corresponds to a near E_f *d* band with 1D character, as seen in the band-structure plot shown in the inset of Fig. 1. Interestingly, formation of such 1D-like chains has been observed in spinels such as ZnV_2O_4.[16] In the case of Ir, due to the extended character of the 5*d* orbital the direct overlap of t_{2g} orbitals which point to each other along a chain direction is large, giving rise to a bandwidth of about 4 eV or so. The crystal field split Ir-e_g separated by an energy gap of 1 eV from the Ir-t_{2g} state remains empty confirming the 3.5+ valence of Ir, with Cu in the monovalent and S in the divalent state. In moving to the low-temperature DOS, while the general features of the DOS remain more or less the same between the HT and LT, significant changes happen close to E_f. The structural data at the LT phase show presence of two distinct classes of Ir ions, one with alternating Ir-Ir short and long bonds and another with uniform Ir-Ir bond lengths. Plotting the DOS projected on these two kinds of Ir ions, referred to as *dimerized* and *nondimerized*, one finds the formation of occupied bonding and unoccupied antibonding-like states close to E_f for dimerized Ir's. Due to the finite mixing of states between *dimerized* and *nondimerized* Ir's in actual crystal structure, the projected DOS on undimerized Ir's also exhibits this feature with larger weight on bonding subbands compared to antibonding subbands. The bonding-antibonding feature, however, is more pronounced with almost equal weights between bonding and antibonding subbands for dimerized Ir's. This leads to charge disproportionation between undimerized and dimerized Ir ions with charges $5.5+\delta$ and $5.5-\delta$ with $\delta=0.05$. Such small difference in charges may be contrasted with a 3*d* transition metal oxide system like Ti_4O_7 (Ref. 17) where the charge disproportionation is found to be nearly complete with Ti's in 3+ and 4+ states. This special feature points to a very delocalized character of Ir together with 1D-like properties.[18] The bonding-antibonding splitting originated due to bond tetramerization in Ir chains with an alternation of $Ir^{3.5-\delta}/Ir^{3.5-\delta}/Ir^{3.5+\delta}/Ir^{3.5+\delta}/\cdots$ gives rise to a gapped solution of electronic structure with GGA as is evident from the DOS plot in Fig. 1.

The gap value is estimated to be about 0.02 eV in agreement with estimates obtained from photoemission study,[19] thereby proving appropriateness of one electron description within GGA to correctly predict the insulating nature at LT. The gap value, as obtained in GGA, is found to be highly sensitive on the structural details, which is expected since the gap originates from structural changes. The structural parameter used in the present work was obtained from Ref. 20. Use of structural parameters from Ref. 7 leads to a pseudogaplike feature in GGA DOS with a tiny DOS at the Fermi level. In view of this, it would have been preferable to carry out structural optimization. This is, however, hindered by the large unit cell and extremely low symmetry of the low-temperature structure. In order to check the influence of the correlation effect, we have carried out a LDA+*U* calculation with antiferromagnetic spin alignment between Ir sites.[21] This calculation, however, leads to a nonmagnetic solution with vanishingly small magnetic moments ($<0.001\mu_B$) at both the dimerized and undimerized Ir sites, and to a DOS almost identical to that obtained within the GGA approach. This situation may be contrasted to the case of Ti_4O_7 (Ref. 22) for which such an approach gave rise to distinctly different magnetic behavior among Ti^{3+} and Ti^{4+}-like ions. This finding is in contradiction to correlation assisted localized spins at Ir^{4+} ions forming spin singlets,[8] confirming the expectation of the correlation effect to be much weaker in the case of an Iridium-sulphide system with extended, delocalized 5*d* and 3*p* states, compared to 3*d* metal-oxide systems.

Figure 2 shows the various possible optical transitions considering the GGA electronic structure at HT and LT for photonic energy ranging from 0 to 3 eV. While the low energy transitions are dominated by Ir t_{2g}-t_{2g} transitions (marked as I and II), the higher energy transitions (marked as III) primarily originate from Ir t_{2g}-e_g and Cu-*d*-Ir t_{2g} transitions, which are allowed due to appreciable hybridization between S-*p* and cations *d*'s. The further high energy transitions, not shown in the figure, are contributed by the *d*-*p* transitions. In moving from HT to LT structure, marked changes happen in the details of the low energy transitions due to opening of a band gap and formation of bonding and antibonding subbands.

Figure 3 shows the computed reflectivity obtained using the joint DOS and the dipole matrix elements. For the HT phase (top panel in Fig. 3) Drude contribution is added to take into account the intraband transitions due to the metallic character of the electronic structure. The Drude component calculated from the bare plasma frequency as obtained in the band-structure calculation (2.5 eV) gives rise to almost 100% reflectivity at low energy. While the added Drude component suppresses a bit the low energy near E_F Ir t_{2g}-t_{2g} transition

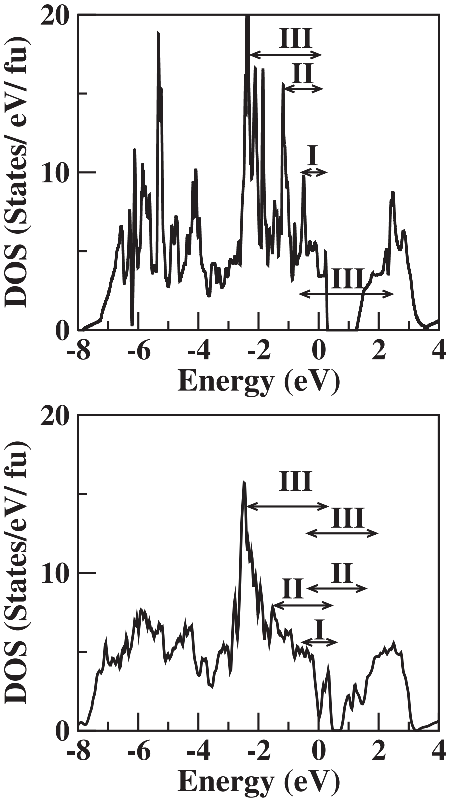

FIG. 2. The various allowed optical transitions for photonic energy ranging from 0–3 eV in the high-temperature and low-temperature phases.

marked as “I” in Fig. 2, it does not mask it completely and traces of it are still visible in the reflectivity spectra. Beside the structure “I,” we find the presence of two other peaks marked as structures “II” and “III,” originating primarily from transitions relating to Ir t_{2g} states appearing far away in energy to near E_F t_{2g} states and Cu-d to Ir-t_{2g} transitions, respectively, with the Ir-t_{2g} to empty Ir-e_g transition contributing to both the structures. Comparing with the experimentally measured spectra, obtained from Ref. 13, as shown in the right-hand upper panel of Fig. 3, we find the computed spectra to be in reasonably good agreement with the experimental spectra, with certain differences in details; e.g., the structure I in experimental spectra is found to be totally masked by the Drude contribution, while structures II and III are shifted a bit to higher energy (by about 0.2 eV) compared to theoretical spectra. Moving to the low-temperature reflectivity spectrum, shown in the bottom panels of Fig. 3, the low-temperature reflectivity drops down to about 60% signaling the insulating character of the LT electronic structure. The structure I becomes more pronounced which in this case is contributed by the transition between Ir bonding and antibonding subbands, while the structures II and III remain more or less similar to the HT structure. The dip preceding structure II is more pronounced in the case of HT spectra compared to LT spectra, which primarily arises due to the fact that the formation of bonding-antibonding bands in LT pushes the quasi-1D-like portion of the t_{2g} manifold more toward the broad filled part of the t_{2g} manifold, compared to the HT electronic structure. This also causes the gap between the Ir t_{2g}-e_g manifold to diminish in the case of LT compared to the HT phase.

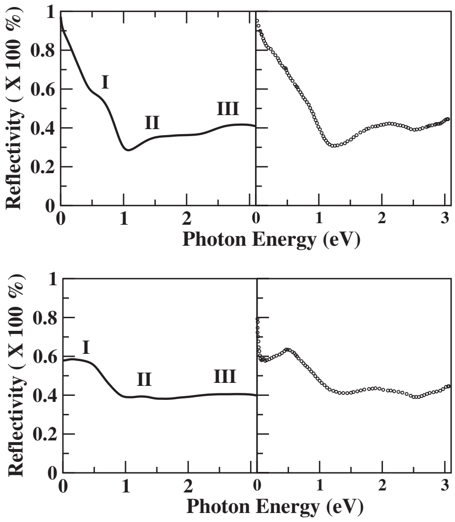

FIG. 3. Calculated reflectivity spectrum (× 100%) (left panels) in comparison with the experimental data (Ref. 13) shown in the right panels for the high-temperature (upper panels) and low-temperature (lower panels) phases. I, II, and III indicate the prominent structures corresponding to optical transitions marked in Fig. 2.

Figure 4 shows the real part of the computed diagonal conductivity for HT and LT crystals (shown in left panels) in comparison with experimental spectra shown in right panels. The diagonal conductivity follows the same trend as the corresponding reflectivity spectra. The structures marked as “α”

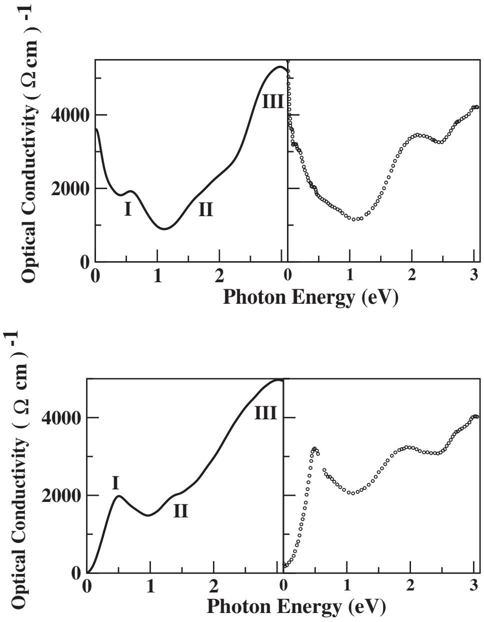

FIG. 4. Absorptive part of the calculated (left panels) diagonal optical conductivity of $CuIr_2S_4$ at high-temperature (top panels) and low-temperature (bottom panels) phases, respectively. The right panels show the experimental data taken from Ref. 13. I, II, and III indicate the prominent structures corresponding to optical transitions marked in Fig. 2.

and "β" in the experimental spectra (Ref. 13) we identify as structures I and II in our calculated spectra, with spectrum II shifted a little bit to lower energy compared to experimental spectra, as already mentioned. While an experimental report in this context[13] associates Ir t_{2g}-e_g transitions to the β/II peak, our first-principles calculations show the β/II peak to originate primarily from the transition related to Ir-t_{2g}-Ir-t_{2g}, with the Ir t_{2g}-e_g transition contributed spectral weight moved mostly to structure III. An optical gap of about 60 meV is obtained from our calculated optical spectrum. This is not apparent in the experimental spectrum presumably because of instrumental broadening. The authors in Ref. 13 arrived at a much larger value from their extrapolation technique of experimental spectra. The dc resistivity measurements, however, have yielded an activation energy which is at the most 47 meV, at a much better agreement with our calculated value of 20 meV, obtained from band structure.

In summary, we have studied the electronic and optical properties of spinel compound $CuIr_2S_4$ at high-temperature and low-temperature phases using the first-principles DFT calculation. Our study finds correlation to play little role. The transition from HT to LT crystal structure with complex ordering pattern, therefore, may be rationalized in terms of formation of one-dimensional bands which gives rise to an *orbitally driven Peierls state*.[12] Our computed reflectivity and conductivity spectra based on the GGA electronic structure are in good agreement with measured spectra. We find the electronic structure to be highly sensitive on the crystal structure data. The observed differences in the details between the theoretical and experimental spectra, we believe, therefore can be improved in terms of better refined crystal structure data at low temperature.

S.S. thanks CSIR for financial support. M.D.R. acknowledges support from DST, Government of India vide Project No. SR/WOS-A/PS-37/2004. T.S.D. acknowledges funding through a Swarnajayanti grant and Advanced Materials Research Unit. The authors acknowledge the input of Sumit Mazumdar and Torsten Clay in the formulation of ideas, through an Indo-U.S. joint network program (Grant No. JC/54/2007/Correlated electrons in materials).

---

[1] A. Damascelli, Z. Hussain, and Z. Shen, Rev. Mod. Phys. **75**, 473 (2003).

[2] C. N. R. Rao, A. K. Cheetham, and R. Mahesh, Chem. Mater. **8**, 2421 (1996).

[3] A. I. Poteryaev, J. M. Tomczak, S. Biermann, A. Georges, A. I. Lichtenstein, A. N. Rubtsov, T. Saha-Dasgupta, and O. K. Andersen, Phys. Rev. B **76**, 085127 (2007).

[4] N. Tsuda, K. Nasu, A. Yanase, and K. Siraton, *Electronic Conduction in Oxide* (Springer-Verlag, Berlin, 1991).

[5] T. Furubayashi, T. Matsumoto, T. Hagino, and S. Nagata, J. Phys. Soc. Jpn. **63**, 3333 (1994).

[6] K. Kumagai, K. Kakuyanagia, R. Endohb, and S. Nagata, Physica C **341-348**, 741 (2000).

[7] P. G. Radaelli, Y. Horibe, M. J. Gutmann, H. Ishibashi, C. H. Chen, R. M. Ibberson, Y. Koyama, Y. S. Hor, V. Kiryukhin, and S. W. Cheong, Nature (London) **416**, 155 (2002).

[8] M. Croft, W. Caliebe, H. Woo, T. Tyson, D. Sills, Y. S. Hor, S. W. Cheong, V. Kirykukhin, and S. J. Oh, Phys. Rev. B **67**, 201102(R) (2003).

[9] C. Sommers and S. Doniach, Solid State Commun. **28**, 133 (1978).

[10] K. Kumagai, S. Tsuji, T. Hagino, and S. Nagata, in *Spectroscopy of Mott Insulator and Correlated Models*, edited by A. Fujimuri and Y. Tokura (Springer-Verlag, Berlin, 1995).

[11] S. Lakkis, C. Schlenker, B. K. Chakraverty, and R. Buder, Phys. Rev. B **14**, 1429 (1976).

[12] D. I. Khomskii and T. Mizokawa, Phys. Rev. Lett. **94**, 156402 (2005).

[13] N. L. Wang, G. H. Cao, P. Zheng, G. Li, Z. Fang, T. Xiang, H. Kitazawa, and T. Matsumoto, Phys. Rev. B **69**, 153104 (2004).

[14] Full-potential LAPW (P. Blaha, K. Schwartz, G. K. H. Madsen, D. Kvasnicka, and J. Luitz, WIEN2K).

[15] T. Oda, M. Shirai, N. Suzuki, and K. Motizuki, J. Phys.: Condens. Matter **7**, 4433 (1995).

[16] S.-H. Lee, D. Louca, H. Ueda, S. Park, T. J. Sato, M. Isobe, Y. Ueda, S. Rosenkranz, P. Zschack, J. Íñiguez, Y. Qiu, and R. Osborn, Phys. Rev. Lett. **93**, 156407 (2004); T. Maitra and R. Valentí, *ibid.* **99**, 126401 (2007).

[17] V. Eyert, U. Schuringenschlögl, and U. Eckern, Chem. Phys. Lett. **390**, 151 (2004).

[18] R. T. Clay, S. Mazumdar, and D. K. Campbell, Phys. Rev. B **67**, 115121 (2003).

[19] J. Matsuno, T. Mizokawa, A. Fujimori, D. A. Zatsepin, V. R. Galakhov, E. Z. Kurmaev, Y. Kato, and S. Nagata, Phys. Rev. B **55**, R15979 (1997).

[20] T. Sasaki, M. Arai, T. Furubayashi, and T. Matsumoto, J. Phys. Soc. Jpn. **73**, 1875 (2004).

[21] The true spin singlet state without any long range order is not possible to achieve within a LDA+U kind of approach. The AFM spin alignment therefore is the closest approximation to assume.

[22] I. Leonov, A. N. Yaresko, V. N. Antonov, U. Schwingenschlögl, V. Eyert, and V. I. Anisimov, J. Phys.: Condens. Matter **18**, 10955 (2006).